ORNL/TM-2023/3005

Molten Salt Reactor Experiment Simulation Using Shift/Griffin

Donny Hartanto
Eva Davidson
Ashley Godfrey
Yan Cao (ANL)
Tingzhou Fei (ANL)
Mauricio Tano-Retamales (INL)

August 2023

OAK RIDGE National Laboratory

ORNL IS MANAGED BY UT–BATTELLE, LLC, FOR THE U.S. DEPARTMENT OF ENERGY

ORNL/TM-2023/3005

Nuclear Energy Advanced Modeling and Simulation

MOLTEN SALT REACTOR EXPERIMENT SIMULATION USING SHIFT/GRIFFIN

Donny Hartanto
Eva Davidson
Ashley Godfrey
Yan Cao (ANL)
Tingzhou Fei (ANL)
Mauricio Tano-Retamales (INL)

Date Published: August 2023

Prepared by
OAK RIDGE NATIONAL LABORATORY
Oak Ridge, TN 37831-6283
managed by
UT-Battelle, LLC
for the
US DEPARTMENT OF ENERGY
under contract DE-AC05-00OR22725

CONTENTS

LIST OF FIGURES

LIST OF TABLES

ABBREVIATIONS

ANL	Argonne National Laboratory
CE	continuous energy
DOE	Department of Energy
INL	Idaho National Laboratory
LWRs	light-water reactors
MOOSE	Multi-Physics Object Oriented Simulation Environment
MSBR	Molten Salt Breeder Reactor
MSR	molten salt reactor
MSRE	Molten Salt Reactor Experiment
NEAMS	Nuclear Energy Advanced Modeling and Simulation
ORNL	Oak Ridge National Laboratory

ACKNOWLEDGMENTS

This research is supported by the Nuclear Energy Advanced Modeling and Simulation (NEAMS) program of the Department of Energy, Office of Nuclear Energy (DOE-NE). This research made use of the resources of the High Performance Computing Center at Idaho National Laboratory, which is supported by the Office of Nuclear Energy of the U.S. Department of Energy and the Nuclear Science User Facilities under Contract No. DE-AC07-05ID14517. The authors would also like to acknowledge the Shift development team, especially Tara Pandya and Matthew Jessee, and the Griffin development team, especially Olin Calvin, for their technical support with this research. The authors thank Tara Pandya and Rike Bostelmann for their technical review of this report.

ABSTRACT

The Department of Energy (DOE)'s NEAMS focuses its efforts on the development of advanced modeling and simulation (M&S) tools for light-water reactors (LWRs) and non–LWRs (i.e., molten salt reactors, high-temperature gas reactors, microreactors, and fast reactors). In the previous fiscal year, the Multiphysics Applications Driver Technical Area funded molten salt reactor (MSR) M&S at Oak Ridge National Laboratory (ORNL) to generate multigroup macroscopic cross sections with Shift for a MSRE 2D lattice model in Griffin. In addition, Shift's capability to calculate gamma dose rates from activated components in the primary exchangers in a molten salt breeder reactor was also demonstrated.

In fiscal year 2023, ORNL generated multigroup macroscopic cross sections using Shift for a 3D MSRE core model. MSRE depletion calculations using Griffin were also demonstrated in this fiscal year. For the depletion calculation, one-group microscopic cross sections for the 3D MSRE core were generated using Shift, and the decay transmutation library from ORIGEN was converted to an ISOXML file, which is required as input in Griffin. Several Monte Carlo codes, such as OpenMC and Serpent, were also used to benchmark and supplement multigroup cross sections generated by Shift. Multigroup libraries were generated with 8 and 20 group structures, and the study found the 8-group structure to be more accurate when comparing Griffin results to continuous energy (CE) Monte Carlo results. The average flux from CE Shift calculations is up to ~6% higher than the CE Serpent calculations because of different values applied for the energy released per fission (κ values). The average flux in the fuel salt calculated by Griffin using cross sections generated with Shift agrees well with the reference CE Shift solution; the same is valid for the corresponding Serpent results. The maximum relative error is ~6% and ~2% compared to the CE Shift and Serpent reference solutions, respectively. Meanwhile, the average flux calculated by Griffin in the graphite moderator shows a higher difference in the thermal range when compared to both reference Monte Carlo solutions; this result suggests a need for improvement in cross section generation for the graphite moderator in the thermal range in both Monte Carlo codes.

Griffin depletion calculations using cross sections from Shift and Serpent were performed and compared against ORIGEN calculations, and the nuclide densities calculated by Griffin were found to be generally in agreement with those of ORIGEN. Because a different approach was taken to calculate the energy released per fission (κ values) in Shift and Serpent, a difference in nuclide densities from differences in the average flux was observed between Griffin using Serpent and Shift cross sections. Griffin calculations with Shift cross sections produced higher average flux in the salt than with Serpent cross sections, leading to higher consumption of ^{235}U and higher production of ^{135}Xe. For time-dependent depletion calculations, cross sections were generated with Serpent, and Griffin's results using these cross sections were compared to CE Serpent depletion results, demonstrating good agreement. The average difference in keff between Serpent and Griffin as a function of burnup is about 155 pcm. Similarly, good agreement with small differences up to ~0.5% was also noticed in the nuclide density of ^{235}U and ^{135}Xe.

More details regarding the methodologies invoked to generate the cross section to make code-to-code comparisons are discussed further in this report. User feedback on Griffin and Shift capabilities that will enhance these calculations is provided in this report for future consideration. The work performed this fiscal year can be extended further for multiphysics coupling of Griffin–Pronghorn/SAM with Mole to study precursor flow and salt chemistry.

1. INTRODUCTION

The US DOE's NEAMS program focuses its efforts on the development of advanced M&S tools for LWRs and non-LWRs (i.e., molten salt reactors, high-temperature gas reactors, microreactors, and fast reactors). As part of this effort, different focus areas within NEAMS seek to implement and test features to enable accurate simulation of various physical phenomena in these reactor types and advanced fuels to be used in these reactors. In the previous fiscal year (FY)[1], the Multiphysics Applications Driver Technical Area funded molten salt reactor modeling and simulation at ORNL to generate multigroup macroscopic cross sections with Shift [2] for a MSRE 2D lattice model in Griffin [3]. Likewise, Shift's capability to calculate gamma dose rates from activated components in the primary exchangers in a Molten Salt Breeder Reactor (MSBR) was also demonstrated. This FY, ORNL continued to generate multigroup macroscopic cross sections using Shift, but now for a 3D MSRE core model provided by Argonne National Laboratory (ANL). In addition, MSRE depletion calculations using Griffin were also demonstrated with training from Idaho National Laboratory (INL). To perform depletion calculations with Griffin, one-group microscopic cross sections were generated using Shift, and the decay transmutation library from ORIGEN [4] was converted to an ISOXML file, which is required as input in Griffin. Several Monte Carlo codes, such as OpenMC [5] and Serpent [6], were also used to benchmark and supplement multigroup cross sections generated by Shift.

This report documents the analyses performed, identifies gaps in capability, and provides feedback to improve the user experience of Shift and Griffin. Section 2 discusses the simplified MSRE benchmark[7] model developed by ANL. The details of the model are discussed in the next Section. Section 3 discusses the multigroup cross section methodology used to generate the ISOXML file for use in Griffin. Section 4 provides results from constant flux and time-dependent depletion calculations performed in Griffin with user feedback. Section 5 provides concluding work and future areas of investigation.

2. MSRE MODEL VALIDATION

The reactor that was modeled in this study is the MSRE that was an experimental molten salt reactor operated at ORNL from 1965 to 1969 and recently has been included in the international handbook of evaluated reactor physics benchmark experiments [7]. An unstructured mesh model of a simplified MSRE benchmark developed by ANL is used in this work. It only contains two mixtures: fuel salt and graphite moderator. The temperature of the fuel salt and graphite are 900°C and 600°C, respectively. The model has an array of 512 graphite moderator stringers and three control rod channels filled with fuel salt in the central region, surrounded by the fuel salt. The model has a radius of 70.485 cm. Meanwhile, the height of the graphite moderator stringer is 220.18 cm, and the fuel salt at the top and bottom of the moderator extends 50 cm above and below the moderator region, respectively. An OpenMC model identical to the unstructured mesh model was also provided to ORNL by ANL. This OpenMC model was converted to Serpent and Shift models, as depicted in Figure 1. The Shift model was developed using the SCALE input format.

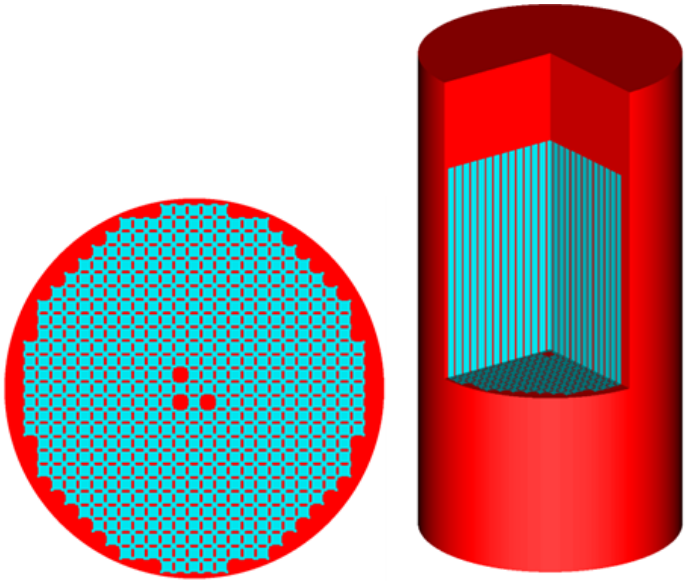

Figure 1. Simplified MSRE Shift model plotted by SCALE/Fulcrum.

Code-to-code comparisons in the effective multiplication factor, k_{eff}, were conducted to confirm that the models were correctly developed, and the results are summarized in Table 1. In each Monte Carlo code, the same version of the nuclear data library, ENDF/B-VII.1, was applied. The thermal scattering library for graphite was also taken into account in the simulation. Each code also utilized the Doppler broadening rejection correction (DBRC) option [8]; the DBRC method is not a default option in OpenMC and Serpent codes. Each calculation used the same parameters: neutron histories per cycle were 500,000, and the total cycles were 450, with 50 inactive cycles.

Two results from Shift are presented using Omnibus-Shift and SCALE-Shift. The Shift Monte Carlo code can be executed via two distinct frontends: SCALE [4] and Omnibus [9]. Currently, cell-wise few-group cross sections can be generated using the Omnibus frontend. Using OpenMC as a reference, the results demonstrate excellent agreement, with a maximum difference of approximately 108 pcm, which suggests that the models have been set up consistently.

Table 1. Comparison of k_{eff} value from several MC codes.

Code	k_{eff}
OpenMC (version 0.13.2)	1.01185 ± 0.00007
Serpent (version 2.2.1)	1.01179 ± 0.00007
Omnibus-Shift (version 7.0.b5)	1.01097 ± 0.00008
SCALE/Shift (version 7.0.b4)	1.01077 ± 0.00009

3. MULTIGROUP CROSS SECTION GENERATION

Once an equivalent MSRE model as the unstructured Griffin mesh was set up in Shift and Serpent, the models were used to generate multigroup cross sections to allow for depletion calculations.

3.1 MACROSCOPIC CROSS SECTION GENERATION

Griffin is a reactor physics code developed and maintained by INL and ANL. It is based on the Multi-Physics Object Oriented Simulation Environment (MOOSE) framework [10] and can be coupled with other MOOSE modules to perform multiphysics analysis of current and advanced nuclear reactors—including steady-state and transient conditions, fuel depletion, fuel performance, irradiation effects on core internals and the reactor pressure vessel, criticality and decay heat calculations, reprocessing, and non-destructive post-irradiation examination [11]. In Griffin, the neutron radiation transport equation is discretized using the finite element method. It can be solved using either diffusion, discrete ordinates (S_N), or spherical harmonics expansion (P_N) methods. A set of multigroup cross sections can be generated for Griffin in an ISOXML format using lattice physics codes or Monte Carlo codes. Macroscopic or microscopic cross sections can be used in Griffin for performing radiation transport calculations, but microscopic cross sections are used in depletion simulations.

In this work, Shift [12] and Serpent [13] were used to generate multigroup macroscopic cross sections to include the following cross sections and parameters required for performing transport calculations: total (Σ_t), fission (Σ_f), absorption (Σ_{abs}), removal (Σ_{rem}), transport (Σ_{tr}), scattering (Σ_s), fission production ($\nu\Sigma_f$), energy release from fission ($\kappa\Sigma_f$), and fission spectrum (χ_p). Few-group cross sections were generated for 20 and 8 groups for fuel salt and graphite moderator at 900°C and 600°C, respectively. The energy structure is summarized in Table 2.

ANL provided ORNL with the 20-group energy structure, and the 8-group energy structure was obtained from Kópházi et al. to solve the time-dependent neutron transport equation for MSRE [14]. The few-group cross sections from Shift and Serpent are typically collapsed from an intermediate multigroup structure that has more energy groups, such as the SCALE 258-group [4, 15], WIMS 172-group [16], or CASMO 70-group [16] structures. For LWRs analysis, the intermediate group structure is usually applied to obtain the leakage-corrected critical spectrum before collapsing to the few-group energy structure. However, because Shift and Serpent use a 3D model for the generation of few-group cross sections for the MSRE, it was considered that the intermediate energy group might be unnecessary. To examine the effect of the intermediate group structure on the accuracy of k_{eff}, the MSRE few-group cross sections were generated by combining numerous intermediate and few-group energy structures, and the results are discussed in the subsequent section 4. The input block for Shift and Serpent for the 8-group macroscopic cross section generation is provided in Appendix A and B.

The 20-group and 8-group cross sections generated by Shift and Serpent are depicted in Figures 2-7, and the differences in the scattering cross section generated by Shift and Serpent are illustrated in Figures 8-9. In general, the cross sections produced by the two codes are in excellent agreement. Some noticeable differences were observed specifically in the last group of Σ_{tr} for graphite moderator and of Σ_{rem} for fuel salt. Different approaches were adopted by each to calculate Σ_{tr} [12, 13]; they are not discussed in this report. On the other hand, the perceptible difference in the last group of Σ_{rem} can be attributed to a substantial discrepancy in the last group of within-group scattering cross section in the fuel salt, as shown in Figure 8. The relative absolute difference between Shift and Serpent for the last within-group scattering is about 50%. Moreover, the 8-group structure in the two codes provides a smaller discrepancy than the 20-group structure. It is also important to note that Shift and Serpent use different data files for κ values, which propagates to slightly different flux values, as discussed in Section 4.

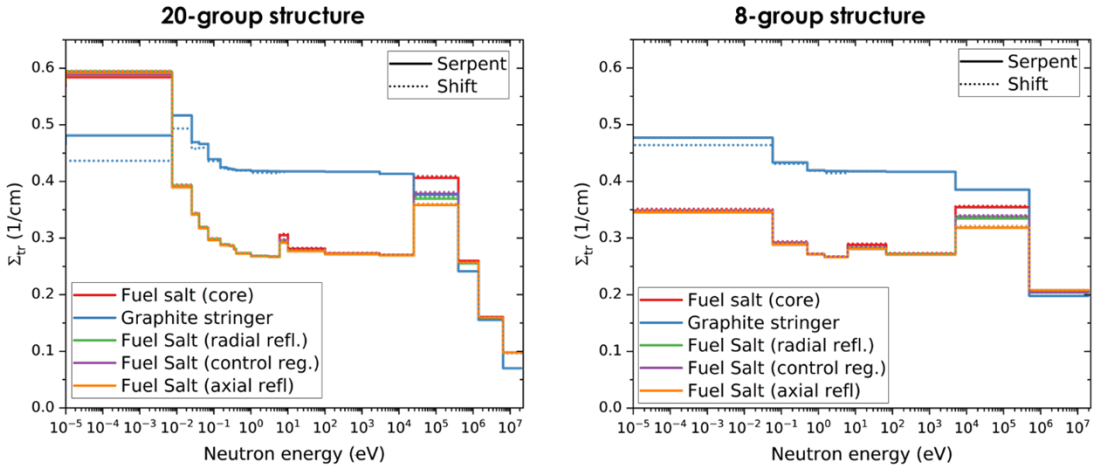

Figure 2. Macroscopic transport cross section.

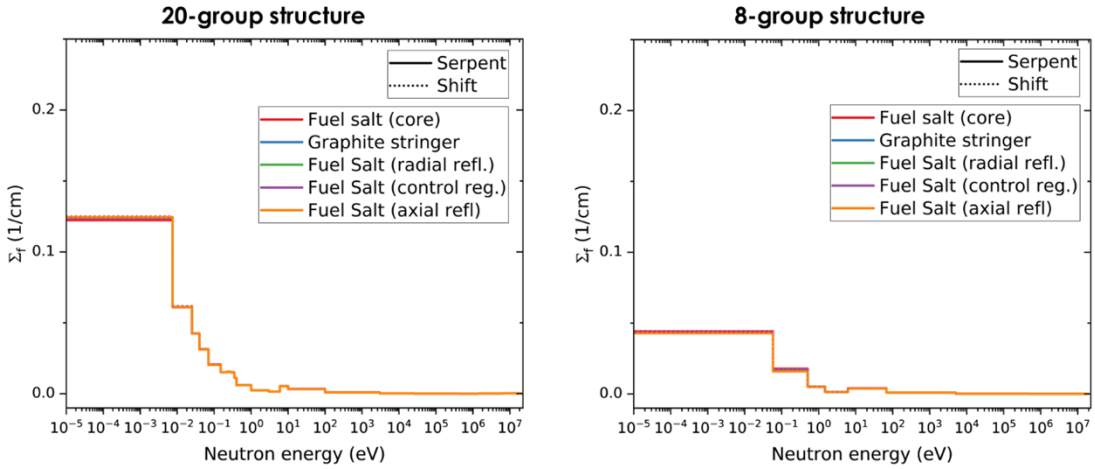

Figure 3. Macroscopic fission cross section.

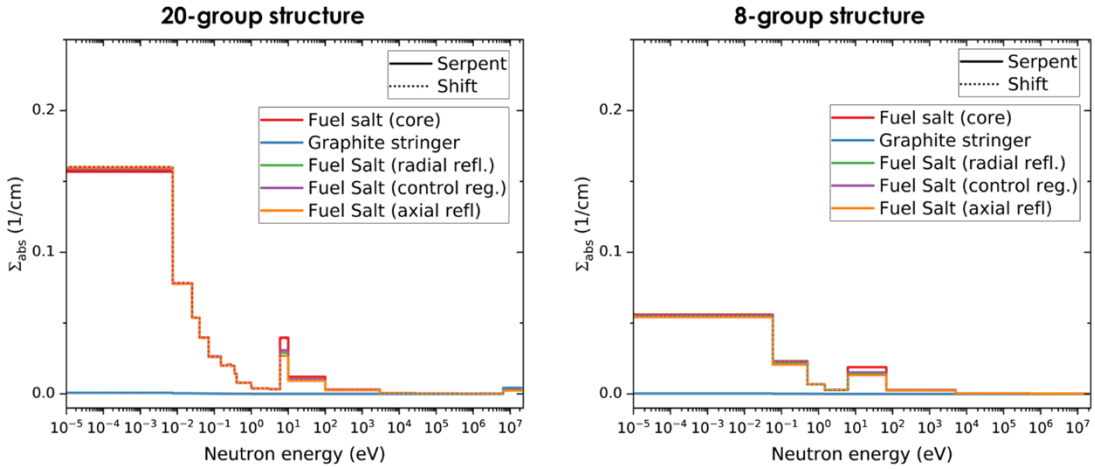

Figure 4. Macroscopic absorption cross section.

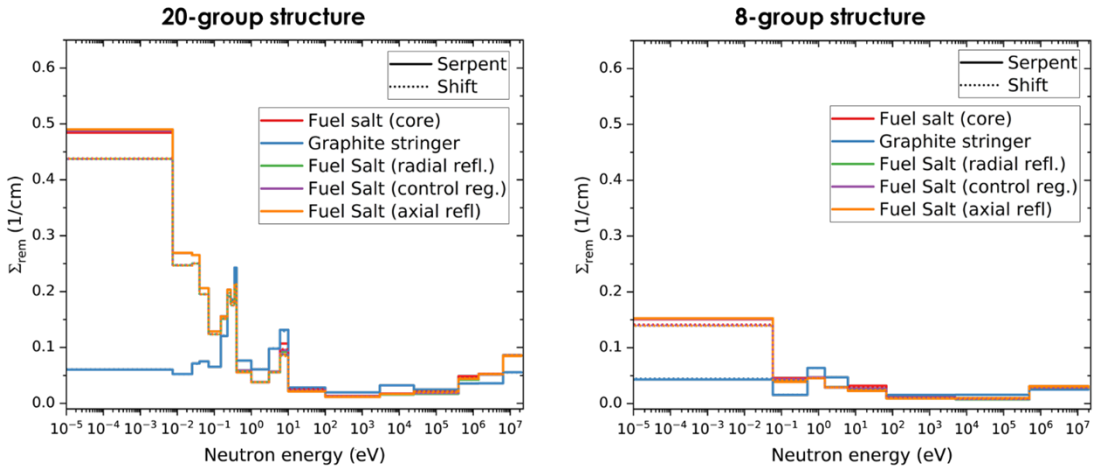

Figure 5. Macroscopic removal cross section.

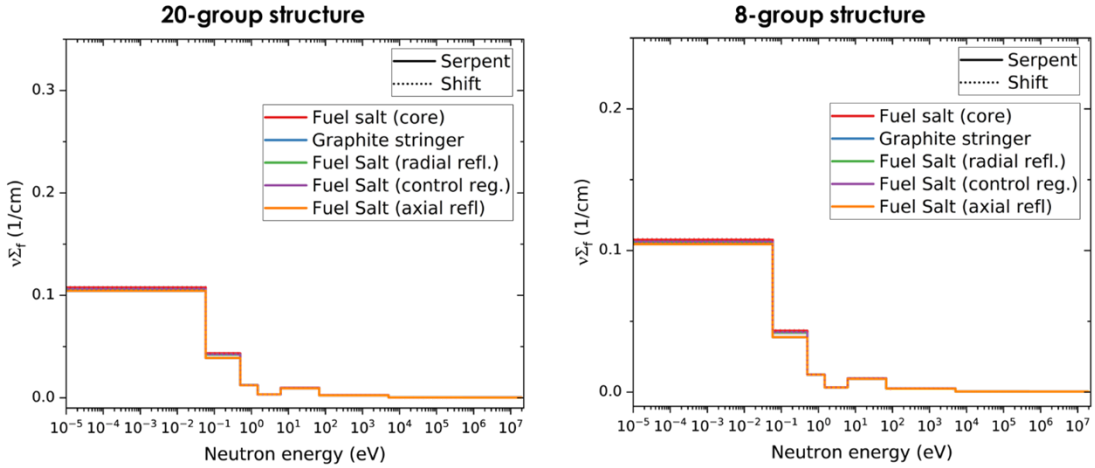

Figure 6. Macroscopic fission production cross section.

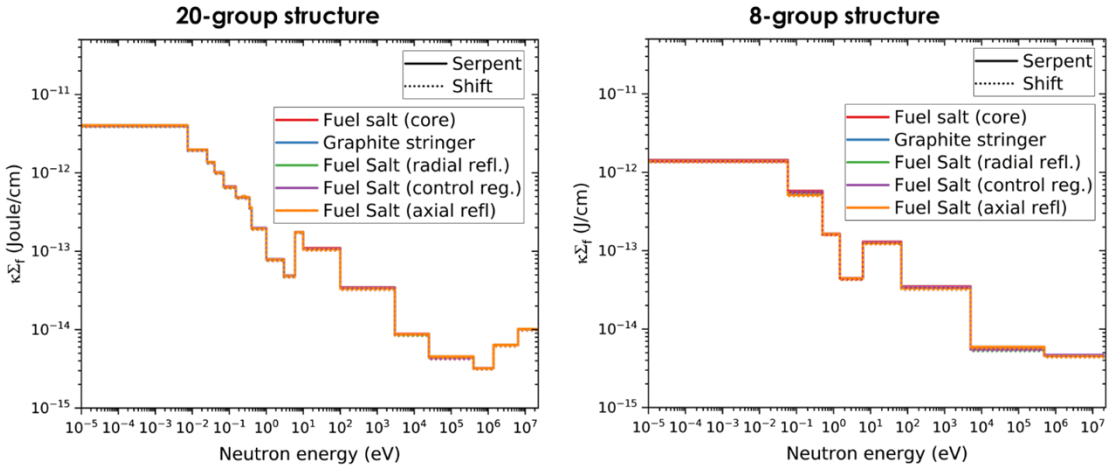

Figure 7. Energy release from fission cross section.

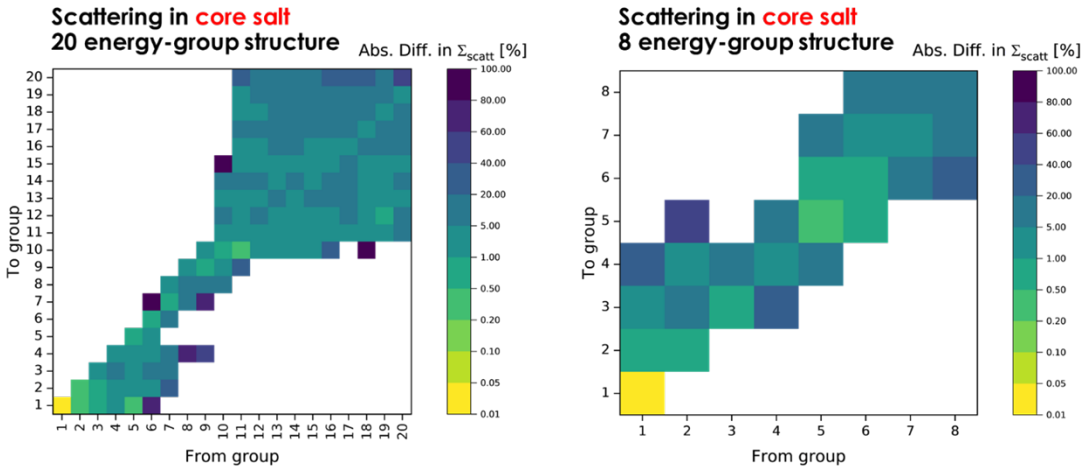

Figure 8. Absolute difference in the scattering cross section of salt in core region between Shift and Serpent.

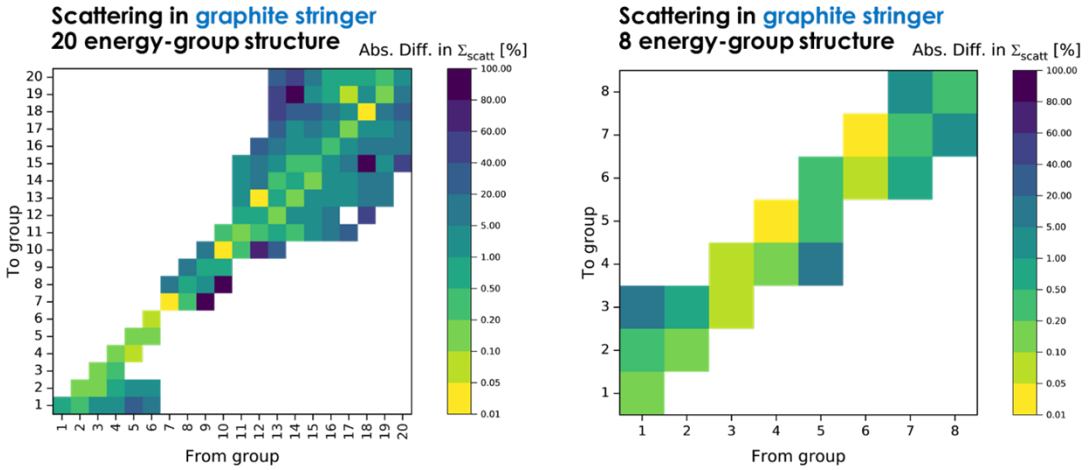

Figure 9. Absolute difference in the scattering cross section of salt in graphite moderator between Shift and Serpent.

Table 2. Multigroup energy structure.

Group	23-group energy (eV)	8-group energy (eV)
0	2.0000E+07	1.9640E+07
1	6.4340E+06	4.9787E+05
2	1.4000E+06	5.0045E+03
3	4.0000E+05	6.7904E+01
4	2.5000E+04	6.1601E+00
5	3.0000E+03	1.4750E+00
6	1.0000E+02	5.0000E-01
7	1.0000E+01	5.8000E-02
8	6.0000E+00	1.0000E-05
9	3.0000E+00	
10	1.0000E+00	
11	4.0000E-01	
12	3.5000E-01	
13	2.7500E-01	
14	2.2500E-01	
15	1.5000E-01	
16	7.0000E-02	
17	4.0000E-02	
18	2.5300E-02	
19	7.5000E-03	
20	1.0000E-05	

3.2 MICROSCOPIC CROSS SECTION GENERATION

Griffin can use microscopic cross sections to solve a steady-state reactor calculation. For such a calculation, a set of microscopic cross section of each nuclide for the same reactions as the macroscopic cross sections is needed, and the atomic density of all nuclides in all materials must be included in the input file. Microscopic cross sections are also required by Griffin to perform depletion calculations. However, additional neutron reaction cross sections summarized in Table 3 are generally required for depletion as well as the decay transmutation library. Current versions of Shift and Serpent do not enable the generation of a complete set of microscopic cross sections, particularly for microscopic transport (σ_{tr}) and scattering (σ_s) cross sections. However, the two codes can produce the microscopic reaction cross sections listed in Table 3 with excellent agreement. The input block is also available in Appendix A and B.

Table 3. Additional microscopic reaction cross sections.

MT	Reaction	MT	Reaction
16	(n, 2n)	101	(n, abs)
17	(n, 3n)	102	(n, γ)
28	(n, np)	103	(n, p)
37	(n, 4n)	104	(n, d)
		105	(n, t)
		106	(n, ^{3}He)
		107	(n,α)
		108	(n, 2α)

4. GRIFFIN CALCULATION

Once the multigroup cross sections are generated, the next step is to run transport and depletion calculations in Griffin; this process is explained further in this section.

4.1 STEADY-STATE CALCULATION

Griffin's steady-state input of 3D MSRE has a structure similar to the 2D MSRE input [1] established in the previous FY, and it is available in Appendix C. The EXODUS-formatted unstructured mesh was imported to Griffin using the [FileMeshGenerator] block. In the [TransportSystems] block, the diffusion solver employing the continuous finite element discretization method (CFEM-Diffusion) and the vacuum boundary condition were chosen to solve the neutron transport equation. Table 4 summarizes the results of Griffin's k_{eff} using the macroscopic cross sections generated from Shift and Serpent, including the effect of using cross sections generated from the intermediate group structure. The difference column displays the discrepancy between Griffin's and the CE Monte Carlo (Shift or Serpent) results used to generate the cross sections. It is observed that the intermediate group structure reduces the accuracy of k_{eff}. Additionally, it is observed that calculations with the 8-group cross sections provide a better agreement with the corresponding CE reference than the 20-group structure. Therefore, all subsequent results in this report use the 8-group structure. It is important to note that using the diffusion method, differences of more than 500 pcm are commonly observed in Monte Carlo calculations because of an incorrect leakage assessment in the diffusion method. The good agreement observed by the 8-group structure in this study may come from error cancellation. Further investigation is suggested for a future study.

Table 4. Effective multiplication factor at steady-state by Griffin.

Code	Intermediate Group	Few Group	k_{eff}	Difference [pcm]
CE Shift	-	-	1.01097 ± 0.00008	-
Shift/Griffin	258	8	1.00482	615
	258	20	1.00013	1084
	172	8	1.00432	665
	172	20	1.00393	704
	8	8	1.01189	-92
	20	20	1.00587	510
CE Serpent	-	-	1.01179 ± 0.00007	-
Serpent/Griffin	172	8	1.00251	928
	172	20	1.00431	748
	8	8	1.01015	164
	20	20	1.00831	348

To further verify the accuracy of the 8-group structure, the average multigroup fluxes in fuel salt and graphite moderator, which are listed in Tables 5 and 6, are also compared between Griffin and the Monte Carlo codes. The [AuxKernels] and [Postprocessors] blocks are set up in the input file to obtain the average flux in Griffin. The neutron fluxes are scaled according to the reactor power (8 MWth) by defining several kernels under the [AuxKernels] block, and the [Postprocessors] block prints them out into the output file. Tables 5 and 6 show that the average flux from CE Shift calculations is higher than the CE Serpent calculations as a result of the

different κ values used in these two codes. Shift considers additional energy released in capture reactions, whereas Serpent considers only the energy deposition from fission (default option in Serpent). Moreover, a similar relative error was observed for the average flux regardless of the intermediate energy group used to generate the few-group cross section. In other words, the accuracy of the flux is not affected by the use of cross sections generated from an intermediate group structure.

Table 5. Average neutron flux in the fuel salt.

Group	CE Shift	Shift/Griffin [258g]*_8g	Shift/Griffin [172g]*_8g	Shift/Griffin 8g	CE Serpent	Serpent/Griffin 8g
1	2.81350E+12	2.82304E+12 (0.34%)	2.82613E+12 (0.45%)	2.81131E+12 (-0.08%)	2.68800E+12	2.63046E+12 (-2.14%)
2	6.26875E+12	6.62991E+12 (5.76%)	6.61475E+12 (5.52%)	6.62103E+12 (5.62%)	5.93369E+12	6.00884E+12 (1.27%)
3	5.39010E+12	5.35070E+12 (-0.73%)	5.35539E+12 (-0.64%)	5.36048E+12 (-0.55%)	5.19569E+12	5.26108E+12 (1.26%)
4	2.10040E+12	2.13978E+12 (1.87%)	2.14205E+12 (1.98%)	2.14325E+12 (2.04%)	2.02112E+12	2.06449E+12 (2.15%)
5	1.00801E+12	1.05104E+12 (4.27%)	1.05240E+12 (4.40%)	1.05279E+12 (4.44%)	9.72770E+11	9.96095E+11 (2.40%)
6	8.37773E+11	8.35354E+11 (-0.29%)	8.34833E+11 (-0.35%)	8.34984E+11 (-0.33%)	8.06246E+11	8.13303E+11 (0.88%)
7	3.19627E+12	3.13849E+12 (-1.81%)	3.11047E+12 (-2.68%)	3.11026E+12 (-2.69%)	3.07824E+12	3.03524E+12 (-1.40%)
8	6.08727E+11	6.10878E+11 (0.35%)	6.19962E+11 (1.85%)	6.19828E+11 (1.82%)	5.84303E+11	5.77152E+11 (-1.22%)

*Intermediate group

Table 5 shows that the average flux calculated by Griffin in the fuel salt agrees well with the reference CE Monte Carlo codes, Shift and Serpent. The maximum relative error is ~6% for the second group compared to the CE Shift reference solution. Meanwhile, the average flux calculated by Griffin in the graphite moderator shows a higher difference in the last two groups when compared to the reference Monte Carlo solution. The maximum relative error of about 10% was observed in the eighth group, which indicates room for improvement in cross section generation in the thermal range for the graphite moderator using both Shift and Serpent.

4.2 DEPLETION CALCULATION

Griffin supports the use of both microscopic and macroscopic cross sections for depletion calculations. Microscopic depletion necessitates microscopic cross sections, and Griffin utilizes the Bateman equation solver to determine the number densities of all pertinent isotopes. The initial number density of each isotope is provided in the input. The macroscopic cross sections necessary for neutron transport calculation are calculated by the mixing operation using the number densities and the microscopic cross sections. The decay transmutation library, which includes the nuclear decay data (i.e., half-lives, decay modes, branching ratios, and recoverable energy per disintegration) and the neutron-induced fission product yield, is also provided.

In contrast, macroscopic depletion uses the macroscopic cross sections that are generated and tabulated in advance on a grid of burnup values among other grids. However, the number densities of the isotopes at each step can also be obtained using the [VectorPostProcessors] block. This block requires the initial number

Table 6. Average neutron flux in the graphite moderator.

Group	CE Shift	Shift/Griffin [258g]*_8g	Shift/Griffin [172g]*_8g	Shift/Griffin 8g	CE Serpent	Serpent/Griffin 8g
1	6.87218E+12	6.94498E+12 (1.06%)	6.94899E+12 (1.12%)	6.92059E+12 (0.70%)	6.57342E+12	6.685230e+12 (1.70%)
2	1.42060E+13	1.40946E+13 (-0.78%)	1.40720E+13 (-0.94%)	1.40606E+13 (-1.02%)	1.35173E+13	1.358052e+13 (0.47%)
3	1.26147E+13	1.27586E+13 (1.14%)	1.27602E+13 (1.15%)	1.27512E+13 (1.08%)	1.21021E+13	1.213908e+13 (0.31%)
4	5.99392E+12	6.01534E+12 (0.36%)	6.01877E+12 (0.41%)	6.01573E+12 (0.36%)	5.74871E+12	5.707317e+12 (-0.72%)
5	3.19138E+12	3.13612E+12 (-1.73%)	3.13829E+12 (-1.66%)	3.13670E+12 (-1.71%)	3.07707E+12	3.044612e+12 (-1.05%)
6	2.67811E+12	2.62786E+12 (-1.88%)	2.62419E+12 (-2.01%)	2.62305E+12 (-2.06%)	2.57430E+12	2.527377e+12 (-1.82%)
7	1.24827E+13	1.17168E+13 (-6.14%)	1.15989E+13 (-7.08%)	1.15973E+13 (-7.09%)	1.20210E+13	1.129502e+13 (-6.04%)
8	2.69948E+12	2.41743E+12 (-10.45%)	2.45701E+12 (-8.98%)	2.45744E+12 (-8.97%)	2.59686E+12	2.367414e+12 (-8.84%)

*Intermediate group

density, the decay transmutation library, and a one-group microscopic reaction cross section (for the reaction listed in Table3). The one-group flux calculated by the neutron transport solver is transferred to this block to solve the Bateman equation.

Ideally, the microscopic depletion approach is preferred. However, this approach is not used here because of limitations in Shift and Serpent's ability to produce a complete set of microscopic cross sections. The two codes can generate the microscopic neutron reaction cross sections with a defined reaction MT number, but they are unable to generate microscopic transport and scattering cross sections. Furthermore, microscopic depletion in Griffin requires the ability to consider the fractional removal of fission products and continuous feed of makeup fuel, which is usually needed to simulate the depletion of a molten salt reactor, but is not yet available when using Griffin's microscopic depletion capabilities. In contrast, fission product removal has been implemented in the [VectorPostProcessors] block [17] for macroscopic depletion with Griffin. For these reasons, the macroscopic depletion approach in conjunction with the [VectorPostProcessors] block was selected in this work to account for removal of fission products.

The macroscopic cross sections for the MSRE depletion were calculated by factoring in the fractional removal of fission products throughout its 375-day operation. The removal rate of gaseous fission products such as Xe and Kr is 4.067E-05/s, whereas the removal rate of the soluble and insoluble metals, including Se, Nb, Mo, Tc, Ru, Rh, Pd. Ag, Sb, and Te, is 8.777E-03/s [18]. Because the current version of Shift is incapable of simulating the fractional removal of fission products, Serpent was utilized to generate the time-dependent macroscopic cross sections. Meanwhile, the one-group microscopic cross sections for the [VectorPostProcessors] block were obtained from Shift and Serpent. The decay transmutation library was created by converting the ORIGEN decay and yields file [4] to ISOXML format. Two different cases of macroscopic depletion were considered: constant flux and time-dependent flux.

4.2.1 CONSTANT FLUX DEPLETION

In the constant flux depletion approach, the Bateman equation solver uses the average flux in the fuel salt calculated at the beginning of the cycle. Two Griffin input files are required. The first input solves the neutron diffusion equation to obtain the average flux in the salt. The second input, which contains the [VectorPostProcessors] block, then employs the average flux in the salt to compute the nuclide densities of the isotopes by solving the Bateman equation. The average flux can be transferred manually (standalone) or automatically using the [MultiApps] block in both inputs. The standalone procedure is comparable to the ORIGEN procedure in which the user inputs the irradiation flux. On the other hand, in the [MultiApps] procedure, Griffin handles the data transfer from the first block of the calculation to the second. The [MultiApps] block is defined in the first input, and the transferred variable is defined in the [AuxVariables] block of the second input. A snapshot of the [MultiApps] input block is provided below, in which the variable 'average_salt_flux' is transferred from the first input to the second input.

```
[First Input]
[MultiApps]
  [dep]
    type = FullSolveMultiApp
    input_files = 'msre_depl.i'
    execute_on = 'final'
  []
[]

[Transfers]
  [flux_dep]
    type = MultiAppVariableValueSampleTransfer
    to_multi_app = dep
    source_variable = 'average_salt_sflux'
    variable = 'average_salt_sflux'
  []
[]

[Second Input]
[AuxVariables]
  [average_salt_sflux]
  []
[]
```

The evolution of several isotopes, such as ^{235}U and ^{135}Xe, as a function of operating days using constant flux depletion is depicted in Figures 10-13. For reference, ORIGEN was also used to generate results using the average flux obtained from the CE Monte Carlo solution. Griffin utilized the 8-group macroscopic and 1-group microscopic cross sections generated by both Shift and Serpent. The nuclide densities calculated by Griffin were found to be generally in agreement with those of ORIGEN. One reason for the difference in nuclide densities can be attributed to the difference in the average flux observed when running Griffin with Serpent cross sections and Griffin with Shift cross sections. However, a major cause for the differences is likely due to the different κ values used in Shift and Serpent. Shift cross sections yield a higher average flux in the salt than Serpent cross sections and, consequently, a higher consumption of ^{235}U and a higher production of ^{135}Xe. Lastly, the results generated with the standalone procedure were found to be in agreement with the [MultiApps] procedure.

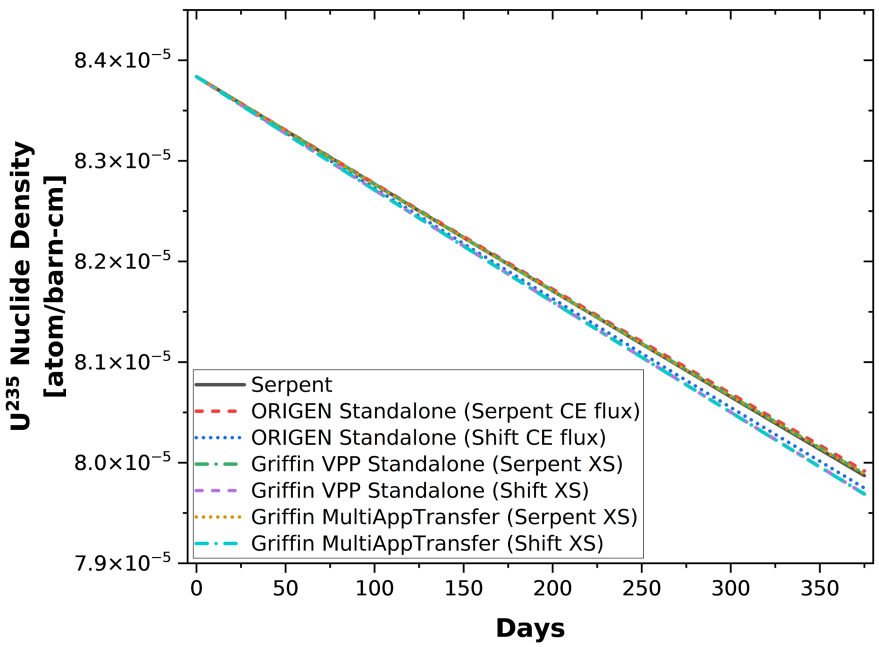

Figure 10. Nuclide density of ^{235}U from constant flux depletion.

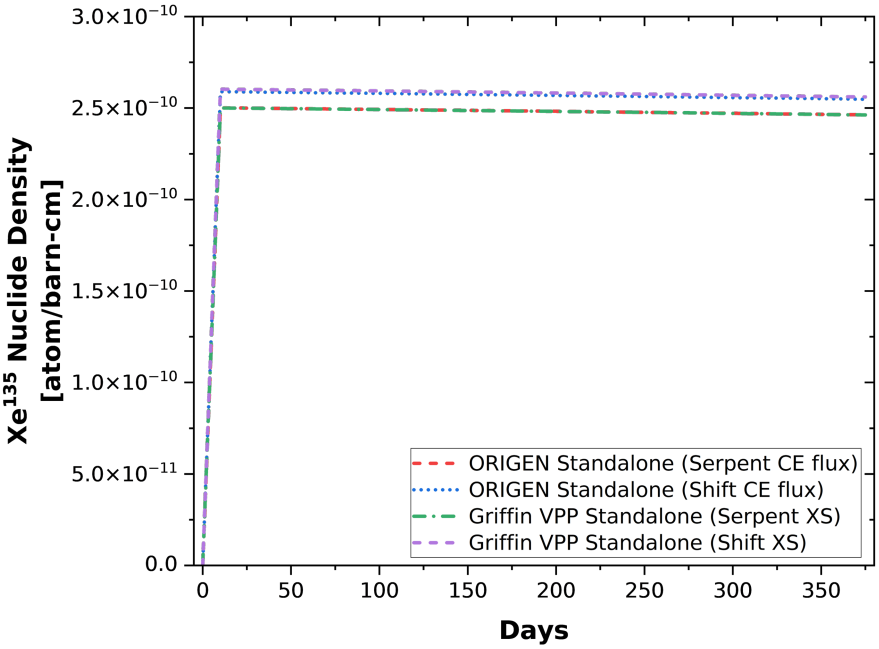

Figure 11. Nuclide density of ^{135}Xe in the fuel salt from constant flux depletion without fission products removal.

4.2.2 TIME-DEPENDENT FLUX DEPLETION

In the time-dependent flux depletion approach, the Bateman equation solver uses the average flux in the fuel salt calculated at each time step. Similar to the constant flux depletion, two Griffin input files are required.

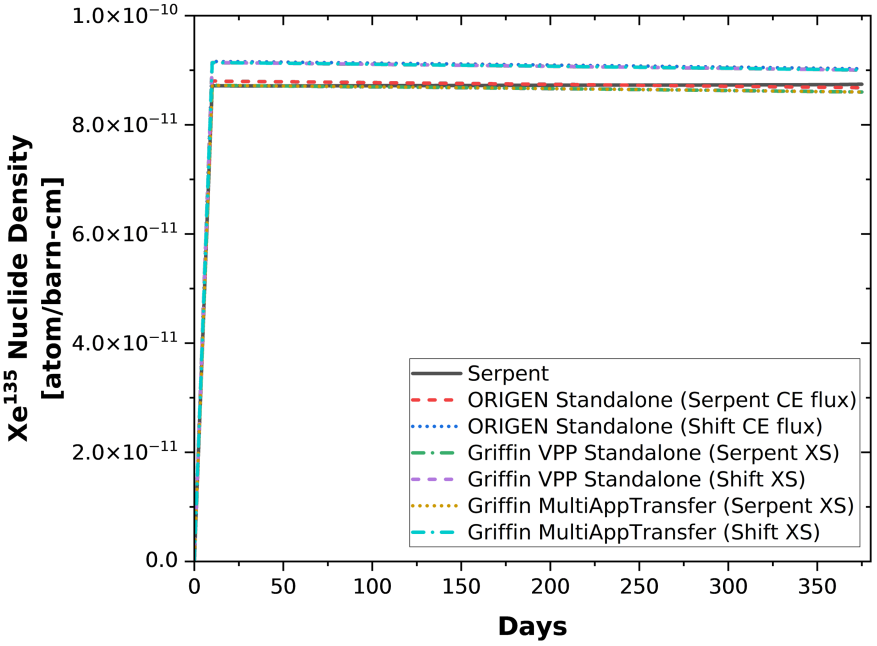

Figure 12. Nuclide density of ^{135}Xe in the fuel salt from constant flux depletion with fission products removal.

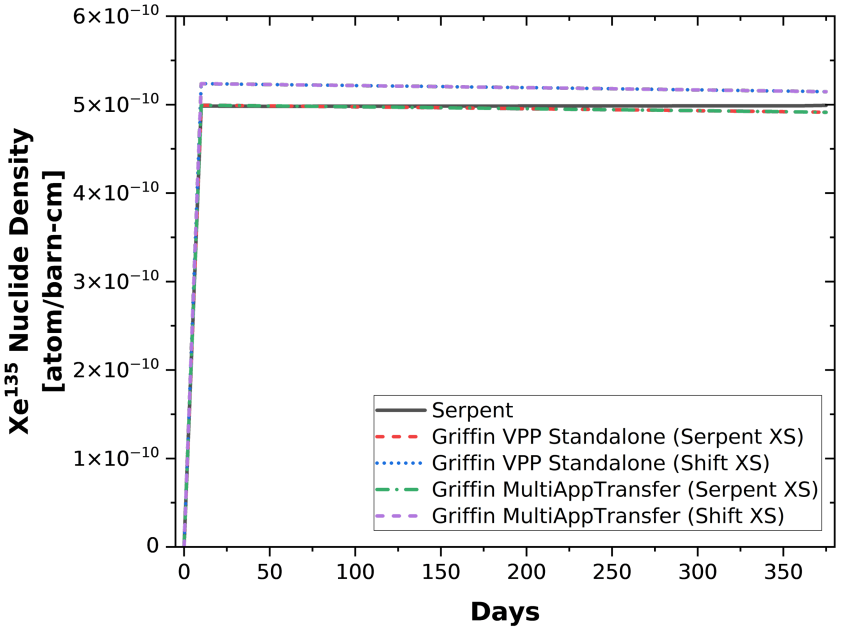

Figure 13. Nuclide density of ^{135}Xe in the off-gas system from constant flux depletion.

The first input contains the neutron solver, and the second input contains the depletion solver. However, a standalone procedure is not suggested for the time-dependent calculation. Instead, the [MultiApps] block was used to pass the average flux from the first input to the second input for each time step.

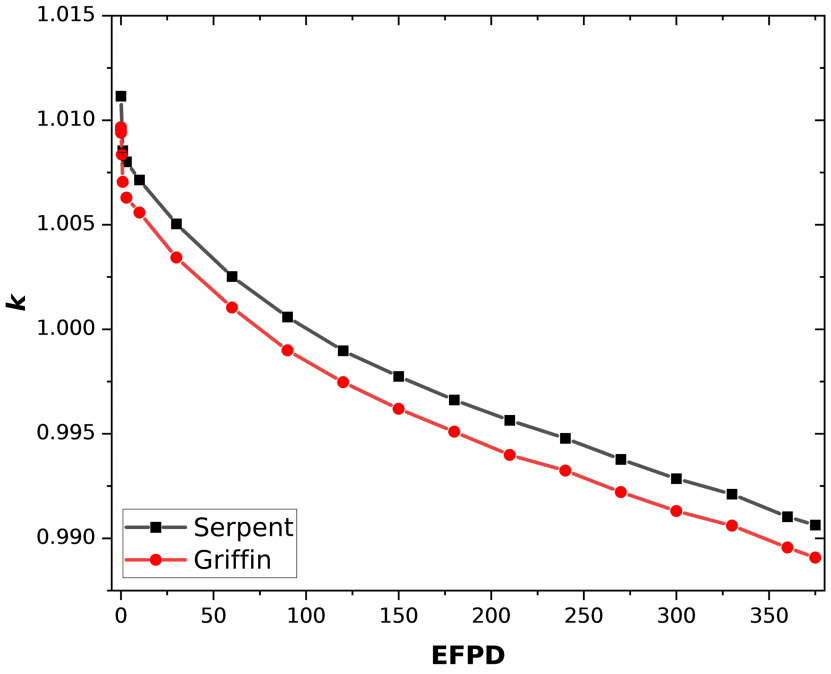

Figure 14. k_{eff} **as a function of burnup.**

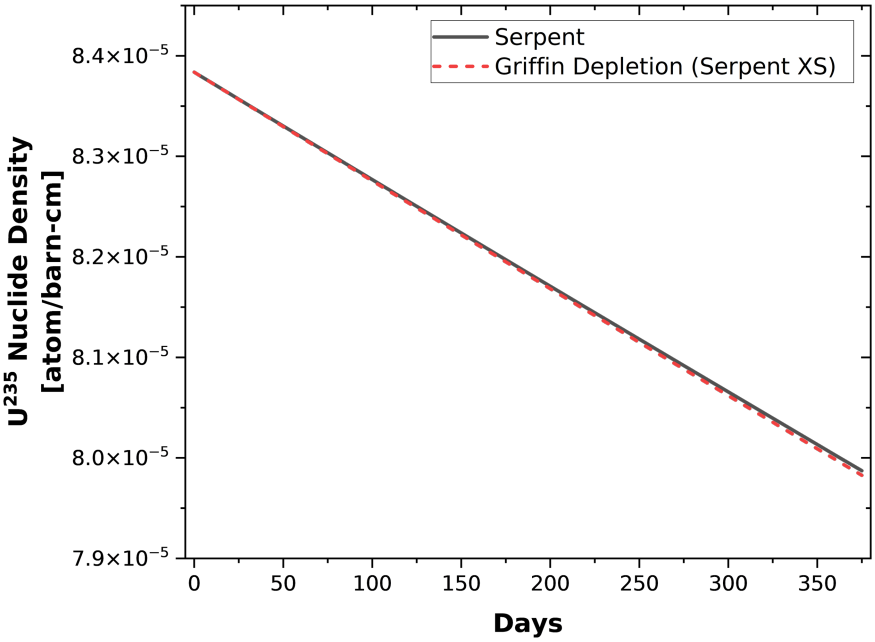

Figure 15. Nuclide density of ^{235}U from time-dependent flux depletion.

Figures 14 to 17 illustrate Griffin's results in the effective multiplication factor and the evolution of several isotopes, such as ^{235}U and ^{135}Xe, as a function of operating days. Griffin used the macroscopic cross section generated by Serpent, which considers the fractional removal of fission products. A similar feature will be available in Shift in the future. Griffin's results are compared to the CE Serpent depletion results, and they

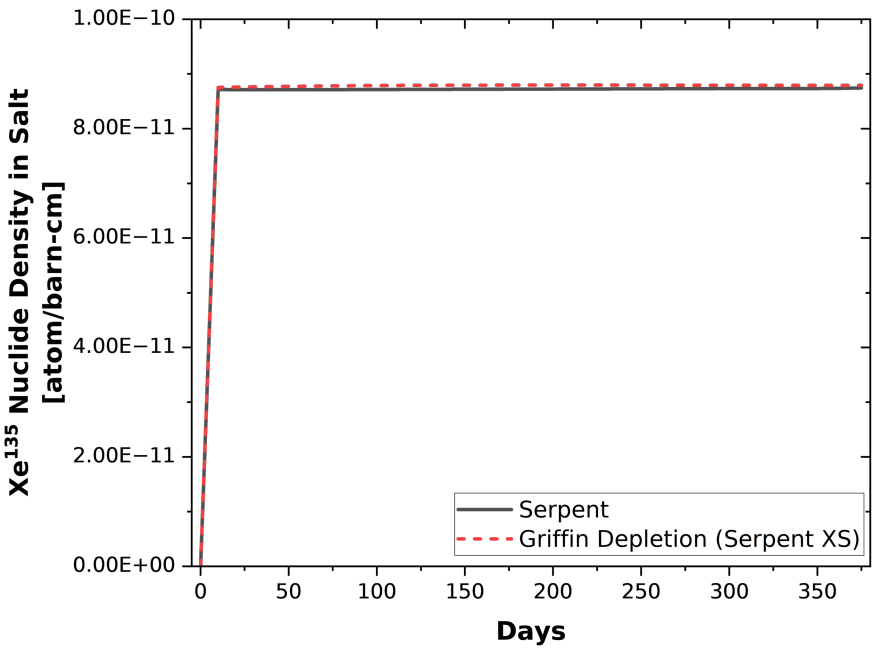

Figure 16. Nuclide density of ^{135}Xe in the fuel salt from time-dependent flux depletion.

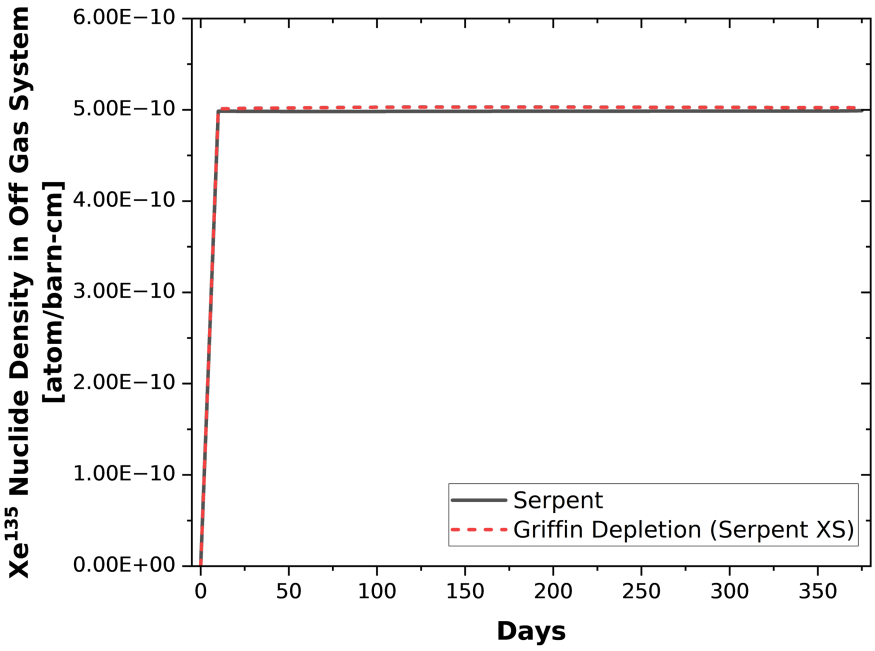

Figure 17. Nuclide density of ^{135}Xe in the off-gas system from time-dependent flux depletion.

are in good agreement. For example, the average difference in keff between Serpent and Griffin as a function of burnup is about 155 pcm. Similarly, good agreement was also observed in the nuclide density of ^{235}U and ^{135}Xe.

4.2.3 USER FEEDBACK

Griffin has been utilized effectively for MSRE depletion calculations. ANL and INL provided substantial assistance to the ORNL team on the Griffin input structure and facilitating access to the recently developed Griffin depletion solver. The teamwork and collaboration on this project enabled independent testing of the newly implemented functionalities in Griffin at ORNL. Griffin can be used to simulate a simple fuel cycle of the MSRE. However, it is suggested that the following features be considered for future development in Griffin.

- Include the fractional removal of fission products and continuous makeup fuel feed as part of the microscopic depletion approach. The current microscopic depletion approach is intended to support only the depletion calculations for solid fuels.
- Permit the definition of multiple waste streams for the fission product removal. Only a single waste stream is accepted in the current Bateman solver.
- For the fractional removal of the fission product, the current Bateman solver necessitates defining each nuclide with its rate. It would be beneficial to enable removal by element to reduce the length of the input.

Additionally, Shift was used to generate the macroscopic and microscopic cross sections for this work. The NEAMS Shift development team also provided substantial guidance and support. Several recommendations were provided to the Shift development team based on the experience of this work.

- Development of the ability to generate a complete set of microscopic multigroup cross sections, including the transport and scattering cross sections.
- Addition of the simulation of fission product fractional removal and continuous makeup fuel feed.

5. CONCLUSIONS

In FY23, ORNL generated multigroup macroscopic cross sections using Shift for a 3D MSRE core model. One-group microscopic cross sections were generated using Shift, and the decay transmutation library from ORIGEN was converted to an ISOXML file required as input in Griffin. Several Monte Carlo codes, such as OpenMC and Serpent, were also used to benchmark and supplement multigroup cross sections generated by Shift. Multigroup libraries were generated with 8- and 20-group structures, and the study found the 8-group structure to be more accurate when comparing Griffin results to the corresponding CE Monte Carlo results. The average flux from CE Shift calculations is higher than the flux from the CE Serpent calculations due to differences in the applied data for the energy released per fission, also known as κ values. The average flux calculated by Griffin in the fuel salt agrees well with the reference Monte Carlo codes, Shift and Serpent. The maximum relative error is ~6% and ~2% compared to the Shift and Serpent reference solutions, respectively. Meanwhile, the average flux calculated by Griffin in the graphite moderator shows a higher difference in the thermal range when compared to the reference Monte Carlo solution, which suggests a need for improvement in cross section generation in the thermal range for both Shift and Serpent. Griffin depletion calculations were run with constant flux and time-dependent flux.

Griffin depletion calculations were performed and compared against ORIGEN calculations, and it is shown that the nuclide densities calculated by Griffin are generally in agreement with those of ORIGEN. A difference in nuclide densities attributed to the difference in the above mentioned average flux was observed between Griffin with Serpent and Shift cross sections. Running Griffin with Shift cross sections yielded higher average flux in the salt than those yielded by Serpent cross sections, leading to a higher consumption of ^{235}U and a higher production of ^{135}Xe. For time-dependent depletion calculations, Griffin results with cross sections generated with Serpent were compared to CE Serpent depletion results, and they were in good agreement. The average difference in k_{eff} between Serpent and Griffin as a function of burnup is about 155 pcm. Similarly, good agreement was seen in the nuclide density of ^{235}U and ^{135}Xe.

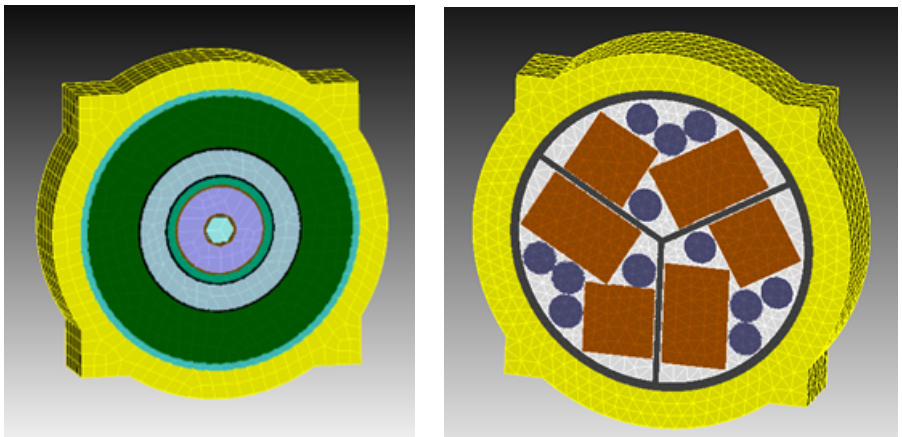

(a) **(b)**

Figure 18. MSRE (a) control rod and (b) basket.

In addition to the cross sections generated and the depletion calculations performed, ORNL also developed a more detailed MSRE mesh that can be used for future multiphysics calculations. Three control rods and the experiment basket (Figure 18) were modeled in addition to the fuel lattice. These regions were combined to generate a 3D full core mesh as shown below in Figure 19. The more detailed mesh can be used to

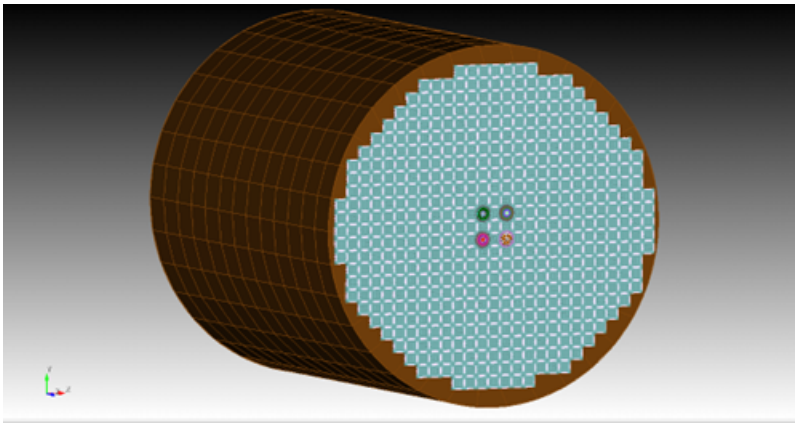

Figure 19. Detailed 3D MSRE mesh.

investigate specific experiments that may have been inserted in the baskets within the MSRE. The multiphysics capability involving Griffin–Pronghorn–Mole can be used to prepare a simulation of the experiment to determine isotopic inventories and compare them to any available experimental data.

In addition to the multiphysics calculations that could be pursued in the future, Shift can be used to investigate gamma heating in the ex-core regions after a reactor is shut down and is in the drained state. This can be used to inform material degradation in the ex-core region using the flux and fluence calculated by Shift using variance reduction methods that enhance the efficiency of the fixed-source calculations.

REFERENCES

[1] E. Davidson, B. Betzler, Y. Cao, and T. Fei, "MSBR Gamma Dose Rate Calculations from Activated Primary Heat Exchanger Compositions," Tech. Rep. ORNL/TM-2022/2582, Oak Ridge National Laboratory, August 2022.

[2] T. M. Pandya, S. R. Johnson, T. M. Evans, G. G. Davidson, S. P. Hamilton, and A. T. Godfrey, "Implementation, capabilities, and benchmarking of Shift, a massively parallel Monte Carlo radiation transport code," *Journal of Computational Physics*, vol. 308, pp. 239–272, 2016.

[3] M. DeHart, F. N. Gleicher, V. Labouré, J. Ortensi, Z. Prince, S. Schunert, Y. Wang, O. Calvin, and J. Harter, "Griffin User Manual," Tech. Rep. INL/EXT-19-54247, Idaho National Laboratory, 2021.

[4] W. Wieselquist and R. A. Lefebvre, "SCALE 6.3.1 User Manual," tech. rep., Oak Ridge National Laboratory, 2 2023.

[5] P. K. Romano, N. E. Horelik, B. R. Herman, A. G. Nelson, B. Forget, and K. Smith, "Openmc: A state-of-the-art monte carlo code for research and development," *Annals of Nuclear Energy*, vol. 82, pp. 90–97, 2015.

[6] J. Leppänen, M. Pusa, T. Viitanen, V. Valtavirta, and T. Kaltiaisenaho, "The Serpent Monte Carlo code: Status, development and applications in 2013," *Annals of Nuclear Energy*, vol. 82, pp. 142–150, 2015.

[7] D. Shen, M. Fratoni, G. Ilas, and J. Powers, "Molten-salt reactor experiment (MSRE) zero-power first critical experiment with ^{235}U," Tech. Rep. NEA/NSC/DOC(2006)1, OECD/NEA, 2019.

[8] B. Becker, R. Dagan, and G. Lohnert, "Proof and implementation of the stochastic formula for ideal gas, energy dependent scattering kernel," *Annals of Nuclear Energy*, vol. 36, no. 4, pp. 470–474, 2009.

[9] S. R. Johnson, T. M. Evans, G. G. Davidson, S. P. Hamilton, T. M. Pandya, K. E. Royston, and E. D. Biondo, "Omnibus User Manual," Tech. Rep. ORNL/TM-2018/1073, Oak Ridge National Laboratory, 2020.

[10] A. D. Lindsay, D. R. Gaston, C. J. Permann, J. M. Miller, D. Andrš, A. E. Slaughter, F. Kong, J. Hansel, R. W. Carlsen, C. Icenhour, *et al.*, "2.0-moose: Enabling massively parallel multiphysics simulation," *SoftwareX*, vol. 20, p. 101202, 2022.

[11] https://griffin-docs.hpcondemand.inl.gov/latest/index.html. Accessed: July 2023.

[12] T. M. Pandya, F. Bostelmann, M. Jessee, and J. Ortensi, "Two-step neutronics calculations with shift and griffin for advanced reactor systems," *Annals of Nuclear Energy*, vol. 173, p. 109131, 2022.

[13] J. Leppänen, M. Pusa, and E. Fridman, "Overview of methodology for spatial homogenization in the serpent 2 monte carlo code," *Annals of Nuclear Energy*, vol. 96, pp. 126–136, 2016.

[14] J. Kópházi, D. Lathouwers, and J. Kloosterman, "Development of a three-dimensional time-dependent calculation scheme for molten salt reactors and validation of the measurement data of the molten salt reactor experiment," *Nuclear science and engineering*, vol. 163, no. 2, pp. 118–131, 2009.

[15] K. S. Kim, A. M. Holcomb, R. Bostelmann, D. Wiarda, and W. Wieselquist, "Improvement of the SCALE-XSProc Multigroup Cross Section Processing Procedure for High-Temperature Gas-Cooled Reactor Analysis," Tech. Rep. ORNL/SPR-2020/1429, Oak Ridge National Laboratory.

[16] https://serpent.vtt.fi/mediawiki/index.php/Pre-defined_energy_group_structures. Accessed: July 2023.

[17] S. A. Walker, A. Abou Jaoude, O. W. Calvin, and M. E. Tano Retamales, "Implementation of isotopic removal capability in Griffin for multi-region MSR depletion analysis," *Transactions of American Nuclear Society*, vol. 127, pp. 976–979, 2022.

[18] A. Lo, R. Bostelmann, D. Hartanto, B. Betzler, and W. Wieselquist, "Application of scale to molten salt fueled reactor physics in support of severe accident analyses," Tech. Rep. ORNL/TM-2022/1844, Oak Ridge National Laboratory, 2022.

APPENDIX A. EXAMPLE OF SHIFT INPUT FILE

APPENDIX A. EXAMPLE OF SHIFT INPUT FILE

```
[PROBLEM]
name    "MSRE ANL OpenMC model"
mode    kcode

[MODEL=SCALE]
input  msre_csas6.inp
volume_cells  1.1   1.2   1.3   1.4   1.5   1.6   1.7
              1.8   1.9   1.10  1.11  1.12  1.13  1.14
              2.1
              3.1
              10.1 10.3
volumes       1.4390831E+06 3.0843182E+05 1.7660207E+04 1.7660207E+04
              1.7660207E+04 1.7660207E+04 1.7660207E+04
              1.7660207E+04 1.7660207E+04 1.7660207E+04 8.9942695E+04
              8.9942695E+04 8.9942695E+04 8.9942695E+04
              3.9440255E+05
              1.3175199E+04
              7.8039286E+05 7.8039286E+05

[PHYSICS=ce]
ce_lib ce_v7.1_endf
mode   n
dbrc   true
thermal_energy_cutoff 100

[PHYSICS][BROADEN]
kinematics true

[SOURCE=separable global_fission]
[SOURCE][SHAPE=global]

[SHIFT]
[SHIFT][TRANSPORTER]
verbosity none

[SHIFT][KCODE]
num_histories_per_cycle  500000
num_cycles  450
num_inactive_cycles  50
initial_keff  1.0
entropy_mesh  automatic

[RUN=mpi]

[TALLY]
[TALLY][CELLNODAL msre_xs_8g]
```

```
description "msre_xs"
fine_neutron_bins   1.9640E+07 4.9787E+05 5.0045E+03 6.7904E+01 6.1601E+00
                    1.4750E+00 5.0000E-01 5.8000E-02 1.0000E-05
coarse_neutron_bins 1.9640E+07 4.9787E+05 5.0045E+03 6.7904E+01 6.1601E+00
                    1.4750E+00 5.0000E-01 5.8000E-02 1.0000E-05
cells_by_homog              1.3:1.4:1.5:1.6:1.7:1.8:1.9:1.10:1.11:1.12:1.13:1.14
                            1.1:1.2
                            2.1
                            3.1
                            10.1:10.3
cells_for_hybrid_scatter_pl 1.3:1.4:1.5:1.6:1.7:1.8:1.9:1.10:1.11:1.12:1.13:1.14
                            1.1:1.2
                            2.1
                            3.1
                            10.1:10.3
cells_for_hybrid_scatter_col 1.3:1.4:1.5:1.6:1.7:1.8:1.9:1.10:1.11:
                            1.12:1.13:1.14:2.1:3.1:10.1:10.3
                            1.1:1.2
pn_order   1

[TALLY][CELL msre_micro_xs]
description “msre_micro_xs”
cells        1.3:1.4:1.5:1.6:1.7:1.8:1.9:1.10:1.11:1.12:1.13:1.14:2.1:3.1:10.1:10.3
reactions    flux
neutron_bins 2.000E+07 1.000E-05
micro_mt_zaid : micro_mt
          h-1   16
          h-1   17
          h-1   18
          h-1   28
          h-1   37
          ...
          ...
       es-255   16
       es-255   17
       es-255   18
       es-255   28
       es-255   37
       es-255   101
       es-255   102
       es-255   103
       es-255   104
       es-255   105
       es-255   106
       es-255   107
       es-255   108

[POST]
```

```
[POST][MG_XS]
mgxs_tally       "msre_xs_8g"
xml_output_file  "shift_isotxs"
xml_lib_name     "ISOTXS-neutron"
xml_lib_desc     "ISOTXS"
griffin_homog_cells 1 2 3 4 5
```

APPENDIX B. EXAMPLE OF SERPENT INPUT FILE

APPENDIX B. EXAMPLE OF SERPENT INPUT FILE

```
set title "msre_3d"

% Surface
surf 1 px  -2.540
surf 2 px   2.540
surf 3 py  -2.540
surf 4 py   2.540
surf 5 sqc  3.556  0     1.524 0.508
surf 6 sqc -3.556  0     1.524 0.508
surf 7 sqc  0      3.556 1.524 0.508
surf 8 sqc  0     -3.556 1.524 0.508
surf 10 inf
surf 41 cyl 0.000  0.000  70.485
surf 51 pz  0.000
surf 52 pz  50.00
surf 53 pz  220.18
surf 54 pz  270.18

% Cell to tally

cell 111 11 fuel_salt -10
cell 112 12 graphite  -10
cell 113  2 fuel_salt -10
cell 114  3 fuel_salt -10
cell 115  4 fuel_salt -10

/******** Radial cells of the reactor ****************/
% Cell
cell 11 1 fill 12   1 -2  3 -4  5  6  7  8
cell 12 1 fill 11  -1     3 -4     6
cell 13 1 fill 11      2  3 -4  5
cell 14 1 fill 11        -3              8
cell 15 1 fill 11            4        7
cell 16 1 fill 11              -5
cell 17 1 fill 11                 -6
cell 18 1 fill 11                    -7
cell 19 1 fill 11                       -8
%cell 20 1 outside -1 -2  3
%cell 21 1 outside  2 -2  3
%cell 22 1 outside           4
%cell 23 1 outside       -3

lat    20   1  0.0 0.0 29 29 5.08
  2 2 2 2 2 2 2 2 2 2 2 2 2 2 2 2 2 2 2 2 2 2 2 2 2 2 2 2 2
  2 2 2 2 2 2 2 2 2 2 2 2 1 1 1 1 1 2 2 2 2 2 2 2 2 2 2 2 2
  2 2 2 2 2 2 2 2 2 1 1 1 1 1 1 1 1 1 1 2 2 2 2 2 2 2 2 2 2
```

```
  2 2 2 2 2 2 2 2 1 1 1 1 1 1 1 1 1 1 1 1 2 2 2 2 2 2 2 2
  2 2 2 2 2 2 2 1 1 1 1 1 1 1 1 1 1 1 1 1 1 2 2 2 2 2 2 2
  2 2 2 2 2 2 1 1 1 1 1 1 1 1 1 1 1 1 1 1 1 1 2 2 2 2 2 2
  2 2 2 2 2 1 1 1 1 1 1 1 1 1 1 1 1 1 1 1 1 1 1 2 2 2 2 2
  2 2 2 2 1 1 1 1 1 1 1 1 1 1 1 1 1 1 1 1 1 1 1 1 2 2 2 2
  2 2 2 1 1 1 1 1 1 1 1 1 1 1 1 1 1 1 1 1 1 1 1 1 1 2 2 2
  2 2 2 1 1 1 1 1 1 1 1 1 1 1 1 1 1 1 1 1 1 1 1 1 1 2 2 2
  2 2 2 1 1 1 1 1 1 1 1 1 1 1 1 1 1 1 1 1 1 1 1 1 1 2 2 2
  2 2 1 1 1 1 1 1 1 1 1 1 1 1 1 1 1 1 1 1 1 1 1 1 1 1 2 2
  2 2 1 1 1 1 1 1 1 1 1 1 1 1 1 1 1 1 1 1 1 1 1 1 1 1 2 2
  2 2 1 1 1 1 1 1 1 1 1 1 1 3 1 3 1 1 1 1 1 1 1 1 1 1 2 2
  2 2 1 1 1 1 1 1 1 1 1 1 1 1 1 1 1 1 1 1 1 1 1 1 1 1 2 2
  2 2 1 1 1 1 1 1 1 1 1 1 1 3 1 1 1 1 1 1 1 1 1 1 1 1 2 2
  2 2 1 1 1 1 1 1 1 1 1 1 1 1 1 1 1 1 1 1 1 1 1 1 1 1 2 2
  2 2 1 1 1 1 1 1 1 1 1 1 1 1 1 1 1 1 1 1 1 1 1 1 1 1 2 2
  2 2 2 1 1 1 1 1 1 1 1 1 1 1 1 1 1 1 1 1 1 1 1 1 1 2 2 2
  2 2 2 1 1 1 1 1 1 1 1 1 1 1 1 1 1 1 1 1 1 1 1 1 1 2 2 2
  2 2 2 1 1 1 1 1 1 1 1 1 1 1 1 1 1 1 1 1 1 1 1 1 1 2 2 2
  2 2 2 2 1 1 1 1 1 1 1 1 1 1 1 1 1 1 1 1 1 1 1 1 1 2 2 2
  2 2 2 2 2 1 1 1 1 1 1 1 1 1 1 1 1 1 1 1 1 1 1 1 2 2 2 2
  2 2 2 2 2 2 1 1 1 1 1 1 1 1 1 1 1 1 1 1 1 1 1 2 2 2 2 2
  2 2 2 2 2 2 2 1 1 1 1 1 1 1 1 1 1 1 1 1 1 1 1 2 2 2 2 2
  2 2 2 2 2 2 2 2 1 1 1 1 1 1 1 1 1 1 1 1 1 1 1 2 2 2 2 2
  2 2 2 2 2 2 2 2 2 1 1 1 1 1 1 1 1 1 1 1 1 1 1 2 2 2 2 2
  2 2 2 2 2 2 2 2 2 2 2 1 1 1 1 1 2 2 2 2 2 2 2 2 2 2 2 2
  2 2 2 2 2 2 2 2 2 2 2 2 2 2 2 2 2 2 2 2 2 2 2 2 2 2 2 2

cell  51   0  fill  4  -41  51 -52
cell  52   0  fill 20  -41  52 -53
cell  53   0  fill  4  -41  53 -54
cell  54   0  outside   41  51 -54
cell  55   0  outside  -51
cell  56   0  outside   54

% --- Fuel (Partially enriched uranium):

mat fuel_salt -2.3243 tmp 900 burn 1 vol 2.469415905E+06
 4009.09c    1.18410E-01
 9019.09c    5.94485E-01
 3006.09c    3.07439E-05
 3007.09c    2.63554E-01
92235.09c    1.00802E-03
92238.09c    2.23617E-03
40090.09c    1.04320E-02
40091.09c    2.27496E-03
40092.09c    3.47733E-03
40094.09c    3.52397E-03
40096.09c    5.67727E-04
```

```
% --- Moderator graphite:

mat graphite -1.86 tmp 600 moder grph 6000
 6000.06c    9.278900e-02

therm grph  grph.06t

% --- boundary condition (1 for vacuum, 2 for reflective):

set bc   1

set dbrc 0.4e-06 210e-06 92235.85c 92238.85c

% --- Generate Macroscopic XS:

set gcu 11 12 2 3 4
set micro 8g
set edepmode 0
ene 8g  1 1.0000E-11 5.8000E-08 5.0000E-07 1.4750E-06 6.1601E-06
          6.7904E-05 5.0045E-03 4.9787E-01 2.0000E+01

% --- Generate MICROSCOPiC XS:
set mdep 11 2.469415905E+06 1 fuel_salt
   10010 16  10010 17   10010 18   10010 28   10010 37   10010 101  10010 102
             10010 103  10010 104  10010 105  10010 106  10010 107  10010 108
   ...
   ...
    992550 16 992550 17  992550 18  992550 28  992550 37  992550 101 992550 102
            992550 103 992550  104 992550 105 992550 106 992550 107 992550 108
ene group1 1 1e-11 2.0e+1

% --- Neutron population and criticality cycles:

set pop 500000 440 60
set nfg 8  5.8000E-08 5.0000E-07 1.4750E-06 6.1601E-06
           6.7904E-05 5.0045E-03 4.9787E-01
set power 8e6
```

APPENDIX C. EXAMPLE OF GRIFFIN INPUT FILE

APPENDIX C. EXAMPLE OF GRIFFIN INPUT FILE

```
# Molten Salt Reactor Experiment
# Griffin Main Application Input
# Steady State Neutronics Model
# Neutron diffusion without delayed precursor source, no equivalence

[Mesh]
 [loader]
  type = FileMeshGenerator
  file ='../../mesh/MSRE_mesh.e'
 []
[]

[TransportSystems]
  particle = neutron
  equation_type = eigenvalue
  G = 8
  VacuumBoundary = '10000 2000 2001'

  [diff]
    scheme = CFEM-Diffusion
    family = LAGRANGE
    order = FIRST

    assemble_scattering_jacobian = true
    assemble_fission_jacobian = true
  []
[]

[Executioner]
  type =  Eigenvalue
  eigen_tol=1.0E-5
  solve_type = 'PJFNK'
  petsc_options_iname = '-pc_type -pc_hypre_type -ksp_gmres_restart '
  petsc_options_value = 'hypre boomeramg 100'
  free_power_iterations = 4  # important to obtain fundamental mode eigenvalue
[]

[Debug]
  print_block_volume = true
[]

[PowerDensity]
  power = 8e6
  power_density_variable = power_density
  integrated_power_postprocessor = total_power
  power_scaling_postprocessor = power_scaling
```

```
  family = MONOMIAL
  order = CONSTANT
[]

[AuxVariables]
  [Tfuel]
    initial_condition = 900.0
    order = CONSTANT
    family = MONOMIAL
  []
  [scaled_sflux_g0]
    family = LAGRANGE
    order = FIRST
  []
  [scaled_sflux_g1]
    family = LAGRANGE
    order = FIRST
  []
  [scaled_sflux_g2]
    family = LAGRANGE
    order = FIRST
  []
  [scaled_sflux_g3]
    family = LAGRANGE
    order = FIRST
  []
  [scaled_sflux_g4]
    family = LAGRANGE
    order = FIRST
  []
  [scaled_sflux_g5]
    family = LAGRANGE
    order = FIRST
  []
  [scaled_sflux_g6]
    family = LAGRANGE
    order = FIRST
  []
  [scaled_sflux_g7]
    family = LAGRANGE
    order = FIRST
  []
[]

[AuxKernels]
  [scale_flux_g0]
    type = ScaleAux
    multiplying_pp = power_scaling
```

```
  source_variable = sflux_g0
  variable = scaled_sflux_g0
  block = '1 2 3 4 5 6 200 201 211 300 301'
[]
[scale_flux_g1]
  type = ScaleAux
  multiplying_pp = power_scaling
  source_variable = sflux_g1
  variable = scaled_sflux_g1
  block = '1 2 3 4 5 6 200 201 211 300 301'
[]
[scale_flux_g2]
  type = ScaleAux
  multiplying_pp = power_scaling
  source_variable = sflux_g2
  variable = scaled_sflux_g2
  block = '1 2 3 4 5 6 200 201 211 300 301'
[]
[scale_flux_g3]
  type = ScaleAux
  multiplying_pp = power_scaling
  source_variable = sflux_g3
  variable = scaled_sflux_g3
  block = '1 2 3 4 5 6 200 201 211 300 301'
[]
[scale_flux_g4]
  type = ScaleAux
  multiplying_pp = power_scaling
  source_variable = sflux_g4
  variable = scaled_sflux_g4
  block = '1 2 3 4 5 6 200 201 211 300 301'
[]
[scale_flux_g5]
  type = ScaleAux
  multiplying_pp = power_scaling
  source_variable = sflux_g5
  variable = scaled_sflux_g5
  block = '1 2 3 4 5 6 200 201 211 300 301'
[]
[scale_flux_g6]
  type = ScaleAux
  multiplying_pp = power_scaling
  source_variable = sflux_g6
  variable = scaled_sflux_g6
  block = '1 2 3 4 5 6 200 201 211 300 301'
[]
[scale_flux_g7]
  type = ScaleAux
```

```
    multiplying_pp = power_scaling
    source_variable = sflux_g7
    variable = scaled_sflux_g7
    block = '1 2 3 4 5 6 200 201 211 300 301'
  []
[]

[Postprocessors]
  [Salt_avg_flux_g0]
    type = ElementAverageValue
    variable = scaled_sflux_g0
    block = '1 2 3 4 5 6 201 211 300 301'
    execute_on = 'initial timestep_end'
  []
  [Salt_avg_flux_g1]
    type = ElementAverageValue
    variable = scaled_sflux_g1
    block = '1 2 3 4 5 6 201 211 300 301'
    execute_on = 'initial timestep_end'
  []
  [Salt_avg_flux_g2]
    type = ElementAverageValue
    variable = scaled_sflux_g2
    block = '1 2 3 4 5 6 201 211 300 301'
    execute_on = 'initial timestep_end'
  []
  [Salt_avg_flux_g3]
    type = ElementAverageValue
    variable = scaled_sflux_g3
    block = '1 2 3 4 5 6 201 211 300 301'
    execute_on = 'initial timestep_end'
  []
  [Salt_avg_flux_g4]
    type = ElementAverageValue
    variable = scaled_sflux_g4
    block = '1 2 3 4 5 6 201 211 300 301'
    execute_on = 'initial timestep_end'
  []
  [Salt_avg_flux_g5]
    type = ElementAverageValue
    variable = scaled_sflux_g5
    block = '1 2 3 4 5 6 201 211 300 301'
    execute_on = 'initial timestep_end'
  []
  [Salt_avg_flux_g6]
    type = ElementAverageValue
    variable = scaled_sflux_g6
    block = '1 2 3 4 5 6 201 211 300 301'
```

```
  execute_on = 'initial timestep_end'
[]
[Salt_avg_flux_g7]
  type = ElementAverageValue
  variable = scaled_sflux_g7
  block = '1 2 3 4 5 6 201 211 300 301'
  execute_on = 'initial timestep_end'
[]
[Grph_avg_flux_g0]
  type = ElementAverageValue
  variable = scaled_sflux_g0
  block = '200'
  execute_on = 'initial timestep_end'
[]
[Grph_avg_flux_g1]
  type = ElementAverageValue
  variable = scaled_sflux_g1
  block = '200'
  execute_on = 'initial timestep_end'
[]
[Grph_avg_flux_g2]
  type = ElementAverageValue
  variable = scaled_sflux_g2
  block = '200'
  execute_on = 'initial timestep_end'
[]
[Grph_avg_flux_g3]
  type = ElementAverageValue
  variable = scaled_sflux_g3
  block = '200'
  execute_on = 'initial timestep_end'
[]
[Grph_avg_flux_g4]
  type = ElementAverageValue
  variable = scaled_sflux_g4
  block = '200'
  execute_on = 'initial timestep_end'
[]
[Grph_avg_flux_g5]
  type = ElementAverageValue
  variable = scaled_sflux_g5
  block = '200'
  execute_on = 'initial timestep_end'
[]
[Grph_avg_flux_g6]
  type = ElementAverageValue
  variable = scaled_sflux_g6
  block = '200'
```

```
    execute_on = 'initial timestep_end'
  []
  [Grph_avg_flux_g7]
    type = ElementAverageValue
    variable = scaled_sflux_g7
    block = '200'
    execute_on = 'initial timestep_end'
  []
[]

[GlobalParams]
  library_file   = '../../xml_xs/shift_isotxs_8g.xml'
  library_name   = ISOTXS-neutron
  plus           = true
  dbgmat         = false
  isotopes       = 'pseudo'
  densities      = '1.0'
  grid_names     = 'Tfuel'
  grid_variables = 'Tfuel'
[]

[Materials]
   [core_fuel_salt]
     type        = CoupledFeedbackNeutronicsMaterial
     block       = '1'
     material_id = '1'
  [../]
  [core_graphite]
     type        = CoupledFeedbackNeutronicsMaterial
     block       = '200'
     material_id = '2'
  [../]
  [radial_fuel_salt_periphery]
     type        = CoupledFeedbackNeutronicsMaterial
     block       = '211'
     material_id = '3'
  [../]
  [control_center_fuel]
     type        = CoupledFeedbackNeutronicsMaterial
     block       = '2 3 4 5 6 201'
     material_id = '4'
  [../]
  [Top_bottom_reflector]
     type        = CoupledFeedbackNeutronicsMaterial
     block       = '300 301'
     material_id = '5'
  [../]
[]
```

```
[Outputs]
  file_base='msre_8g'
  csv = true
  exodus = false
  perf_graph = false
[]
```